INTERNATIONAL JOURNAL of RENEWABLE ENERGY RESEARCH
Aysar Yasin., Vol.9, No.4, December, 2019

Energy Management of a Stand-Alone DC Microgrid Based on PV/Wind/Battery/ Diesel Gen. Combined with Super-Capacitor

Aysar Yasin*‡

*Department of Energy Engineering and Environment, Faculty of Engineering, An-Najah National University, P.O. Box7, 707 Nablus, Palestine

‡ Corresponding Author; Tel: +970 9 2345 115, Fax: +970 9 2345 982, aysar.yasin@najah.edu

Received: 21.10.2019 Accepted:29.11.2019

Abstract- Distributed generation system is a reliable, economical and efficient electrification option that interconnects different energy sources. Small and local distribution generation system including storage systems and load is defined as a microgrid. This paper presents an energy management strategy to supervise the power flows in a stand-alone DC microgrid power generation plant. The plant is composed of: a wind turbine, a photovoltaic generator, a battery storage system and a diesel generator combined with a supercapacitor. The DC microgrid is designed and modeled using Matlab/ Simulink/ SimPowSys™ environment. The supercapacitor is utilized to cover the deficiency of power shortage during the start-up of the diesel generator. It is also utilized to compensate the limitations on the charging/discharging current of the battery. Some performance indexes are considered: the frequency-deviation, the stability of the DC bus voltage and the AC voltage total harmonic distortion (THDv). The performances of the proposed strategy are evaluated by simulation in different operating conditions. Simulation results confirm the effectiveness of the proposed power management strategy: the DC bus voltage keeps almost constant with accepted fluctuations, the normalized frequency deviation is less than 0.01 and THDv is less than 0.04 during all simulation cases. The power flow between the system sources and the load is balanced: the state of charge of batteries and supercapacitors are maintained within the accepted level during all simulation cases. The results show how the supercapacitors solve the problem of slow dynamic of diesel generator during the startup.

Keywords DC-Microgrid, PV, Wind, Diesel-Generator, Super-Capacitor, Energy Management

1. Introduction

The growing concerns about the environmental effect of conventional energy sources, the misgivings of a future shortage of fossil fuel energy and the need to utilize renewable energy sources are all contributing to further utilize distribution power systems instead of centralized power generation. Renewable energy sources (RES) are utilized exceptionally to reduce global warming gases [1]. The distributed generation systems (DGS) based on RES are reliable, sustainable and economically efficient electrification options [2, 3]. A small and local distribution system including generation and load is defined as microgrid [4, 5]. The microgrid may be on-grid or off-grid. The grid-connected microgrid exchange power with the utility, while the off-grid is separated from the utility and normally located in remote areas far away from the grid. The microgrid is mainly categorized as direct-current (DC), alternating-current (AC) and high-frequency alternating current [6]. The DC microgrid is more effective and easy to integrate renewable energy sources with the DC bus, especially after the great progress in the technology of power electronic converters[6, 7]. The quality of the injected power from the DC microgrid after being converted to AC must be high or at least within the accepted range. Three power quality indicators are important: stable voltage that keeps within the recommended range, stable AC frequency, smooth sinusoidal voltage waveform [8]. To ensure those indicators within the accepted range in the standalone DC microgrid, voltage-regulation, power-sharing, and effective storage should be verified [9, 10, 11, 12]. Such a complex system must be appropriately controlled to achieve high productivity and better stability of load supply. More precisely, the power flow among different energy sources in the standalone DC microgrid and the load must be firmly controlled to confirm that all energy is supplied to the loads.

Many researchers have published numerous scientific papers about the control and management of stand-alone DC microgrid. In [13], a control strategy is designed to manage the power flow in an off-grid hybrid system based on PV-wind-battery, the study is verified using Matlab/Simulink, Good power balance is obtained in spite of load fluctuations. In [14], power control of DC microgrid based on PV Energy Generator (PVEG), Diesel Generator (DG) and super-capacitors (SC) is proposed and realized experimentally, the results showed that the strategy is effective and keeps the DC-bus voltage within the accepted range under proposed

operating conditions. In [15], fuzzy logic based energy management of standalone DC microgrid is presented. The system composed of wind energy generator (WEG), PVEG, DG, and battery storage system (BSS). The numerical results ensure good performance and continuity of power supply. In [16], a control strategy based on feedback and feed-forward control loops is proposed for a stand-alone and grid-connected DC microgrid. Various types of nonconventional energy sources and BSS are gathered in the DC bus, the control strategy guarantees long life span of BSS as it is charged under constant current/constant voltage regime, the DC bus voltage is maintained constant and the power is balanced under the only condition which is that the generated power is higher than load demand. In [17], a coordinated and multivariable energy management strategy is proposed to control the energy flow between PVEG, WEG, and BSS. The energy management strategy realizes a constant current- constant voltage charging regime. The load demand is accurately shared between different energy sources and the DC bus is maintained constant. In [18], a DC microgrid based on PVEG, fuel cell and BSS is proposed. The control strategy is divided into device control levels to improve system reliability, system control level to perform energy management between different energy sources, BSS and load. The results show better performance than classical PI control. In [19],dynamic power management of a standalone hybrid system based on PVEG, fuel cell, BSS, and SC is proposed. All sources are connected to DC bus. Different modes and state of charge conditions of battery and SC are proposed. The DC bus voltage is regulated under dynamic changes of load and variations of weather data. In [20], the authors present a fuzzy logic controller to manage energy flow in a standalone DC microgrid based on PVEG and combination of battery and SC as energy storage system. The SC is used for sudden power demand while batteries are used for long term period. The simulation results prove the effectiveness of the proposed fuzzy logic approach. In [21], a power management model for a DC microgrid composed of RES, BSS, and SC is proposed. The control strategy ensures power balance and grid stability even the weather conditions and load demand keep varying. The BSS behaves as a buffer between the flow demanded and the flow provided while the SC maintains grid voltage around the desired value. In [22], the energy management strategy of standalone microgrid based on power flow control that utilizes a hybrid AC/DC structure is proposed. The DC microgrid is composed of PVEG, WEG, and BSS. BSS keeps the DC bus voltage balanced. A DC/AC inverter is used to provide the voltage and frequency references for the AC bus. The energy management strategy is applied to control the SoC-BSS in a certain range, ensure the frequent transition between charge and discharge by the means of output power limitation of the PVEG, switching WEG and well-regulated load. The results show the feasibility and effectiveness of this energy management strategy.

Compared with the mentioned research papers, this paper comes with the following contributions and enhancements: A deterministic approach of energy management strategy of standalone DC microgrid is implemented. Applying a control strategy that is based on balancing DC-bus voltage using WEG/PVEG/load's sharing and PID controllers, which is not implemented in other papers. The DC microgrid is designed and modeled using Matlab-Simulink-SimPowSys™ environment. The DG is utilized as a backup if BSS is discharged. The paper considers the slow dynamic of DG during starting up by utilizing SC which in turn improves the quality of power signal under harsh conditions. This paper utilizes SC also for discharging/charging energy when the deficient/excess power is greater than the capacity of BSS. The control strategy considers the problem of the fast self-discharging problem of SC. a dump load is considered in the system to effectively manage the excess power in case of fully charged BSS and SC. This paper introduces a model for BSS, SC, and DG with validation. Two simulation sets are performed to simulate all possible real cases. Various performance indexes are used.

The study assumes that all cases studied in the simulation represent the real life cases and the fluctuations in weather conditions represent the most challenging circumstances. The study assumes that in case of power deficiency, the load can be limited to the available power. The study assumes that maintaining the DC bus voltage constant is a good indication to power flow balance between the source and the load.

The objective of this paper is to further study and analyze the standalone power systems based mainly on RES. The followed methodology to verify this study is by simulation based on Matlab-Simulink-SimPowSys™. Such complex systems are not easy to assemble in the lab. The accurate simulation analysis will be the basis for practical realization.

2. System Configuration and Modelling

Figure 1 shows the schematic of the considered DC microgrid power plant. The main elements: WEG, PVG, BSS, SC, and DG. They are controlled by independent control systems, and PVEG considers for the maximum power tracking (MPPT). A summary of the parameters of the DC Microgrid components used in this study is given in Table 1.

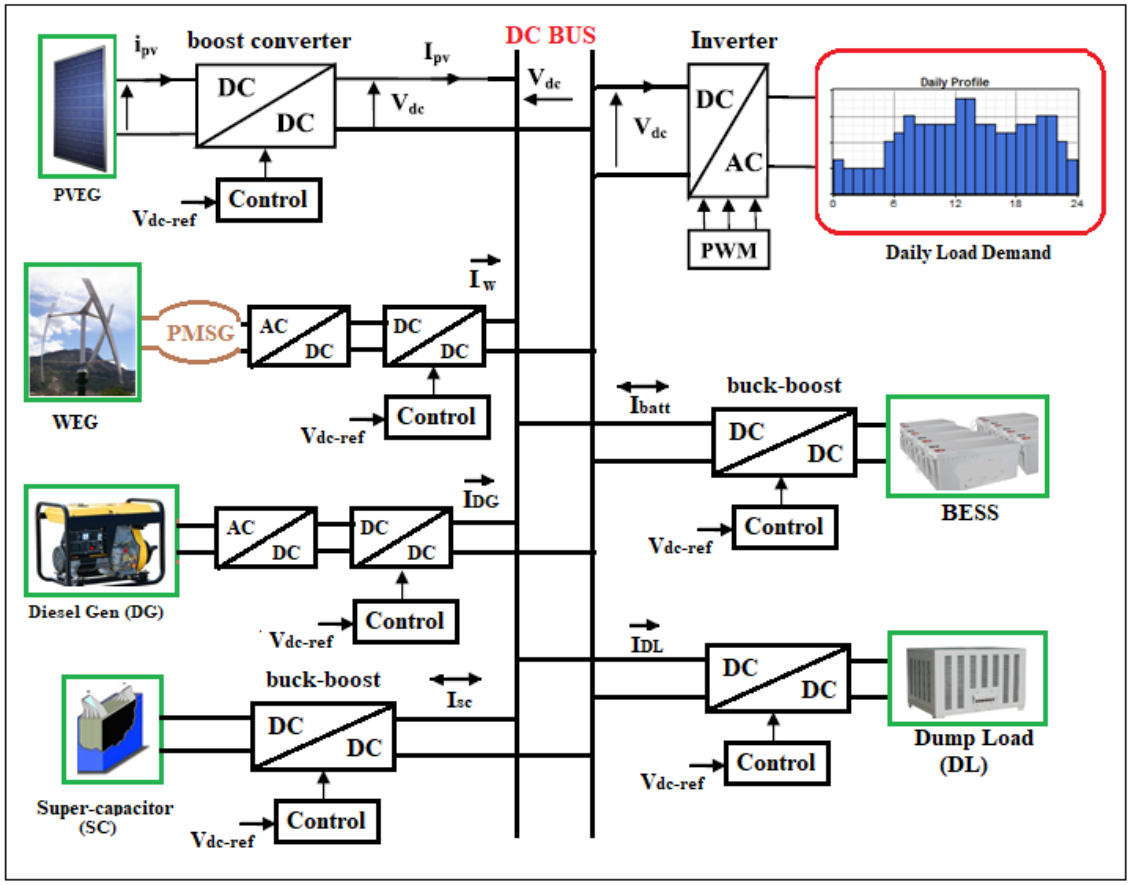

Figure 1. Schematic of standalone DC Microgrid

Table 1: DC-microgrid data

PVEG	
Module-model	Solyndra® - SL001-157
Module-unit	157Wp at STC
Power-rating	1.88kWp
WEG	
Model	TN-1.5 Nozzi Nord (1.5kW)
Cut-in/Cut-out speed	4m/s & 20m/s
Generator type and ratings	1.5kW PMSG @ 50 Hz
DG	
Model	YANIMARL100N
Rated freq. & Voltage	50Hz / 400V
Max Power	3.5kW
SC	
Capacitance	99.5F
Rated Voltage	48V
BSS	
Battery (lead acid)	4.6kWh at 96 V

The mathematical models of the main components are illustrated below:

2.1 PVEG system

The PV cell model used in this study depends on one - diode with the four-parameters model is presented in Figure 2.

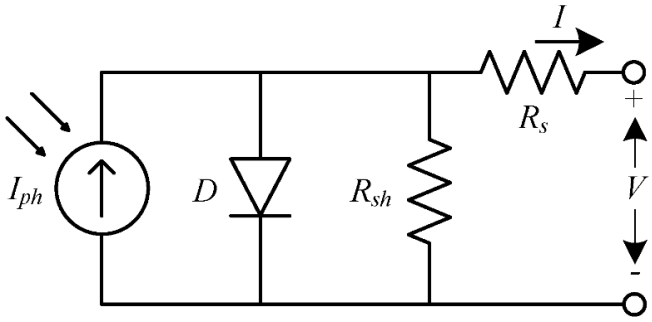

Figure 2. One-diode PV cell with four-parameters model

Details of PVEG model are beyond the purpose of this research.

2.2 WEG system

A vertical axis micro wind turbine with three helical blades has been modeled in this study. The mathematical model of the WEG system is illustrated briefly in equations 1 and 2. The rotors' mechanical power is presented in Equation (1) [23, 24, 25].

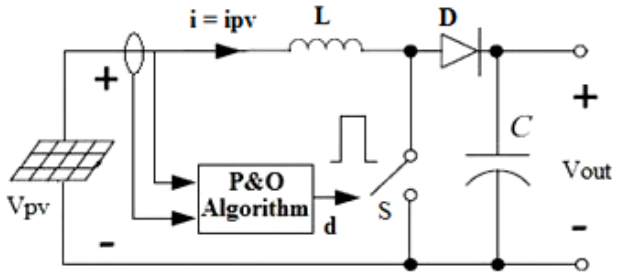

Figure 3. DC/DC boost-converter topology controlled by an MPPT control scheme

$$P_t = \frac{1}{2}\rho a\, C_p\, A_t\, V_w{}^3 \qquad (1)$$

Where At is swept-area of the turbine (m^2), Cp is power-coefficient, **ρ**a is air density (kg/m^3) and V_w is wind velocity (m/s).

The torque T_t on the shaft can be calculated using Equation (2). The rotational speed (Ω) is measured from PMSG's model.

$$T_t = P_t/\Omega = \frac{1}{2}\rho a C_p A_t\, V_w^3/\Omega \qquad (2)$$

Figure 4 shows a schematic of the wind-generator model. Figure 5 shows the validation of WEG. The power generated from WEG differs with respect to wind speed.

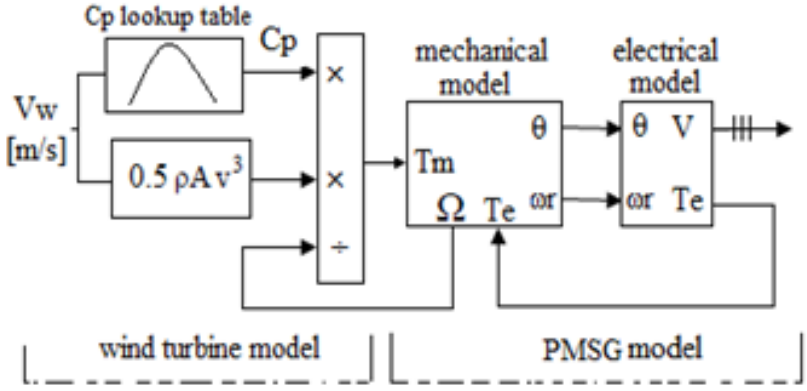

Figure 4. Schematic of the wind-generator model

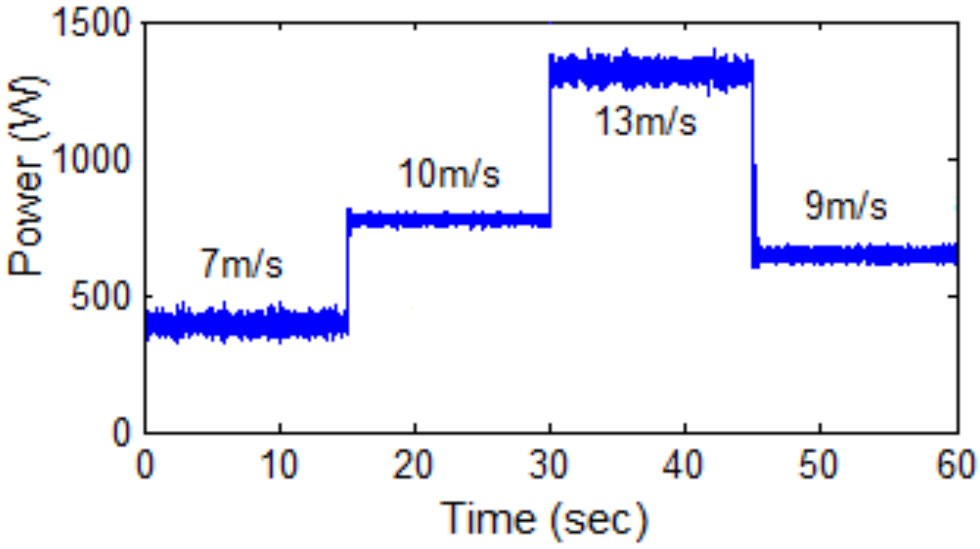

Figure 5. simulation of the wind-generator model

2.3 Diesel Generator –DG

The schematic of DG basic components is presented in Figure 6 [26, 27]. The Matlab-SimPowSys™ simulation diagram of the DG model is presented in Figure 7. It shows electrical and mechanical models. The mechanical side is characterized by the combustion process and engine model. The electrical side is characterized by synchronous-generator and voltage regulation. The model uses tabulated mechanical power data with respect to rotational speed (rad/s) to estimate output mechanical power [26, 27].

The automatic voltage regulator (AVR) is responsible for regulating the excitation voltage of the synchronous generator, it controls the rotor angle and the generator terminal voltage to obtain a good dynamic system and improves the stability [26]. The AVR is classically controlled using the PI controller. The DG is a reliable backup energy source and can offer long-term support, it is frequently used in standalone microgrid

power systems [15, 28, 29, 30, 31]. The output voltage and frequency of DG need several seconds to reach stability because DG has slow dynamic behavior [32]. The validation of the DG model is shown in Figure 8. Figure 8 shows the bad quality of the voltage signal of the DG during the starting up of the DG. The frequency is deteriorated and the voltage amplitude fluctuates. The voltage signal stabilizes after several seconds.

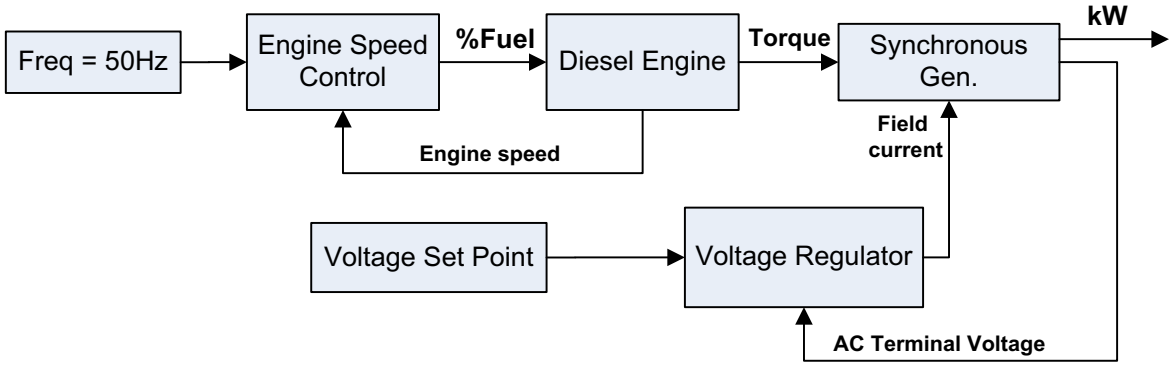

Figure 6. Main functional blocks of DG and their interconnections

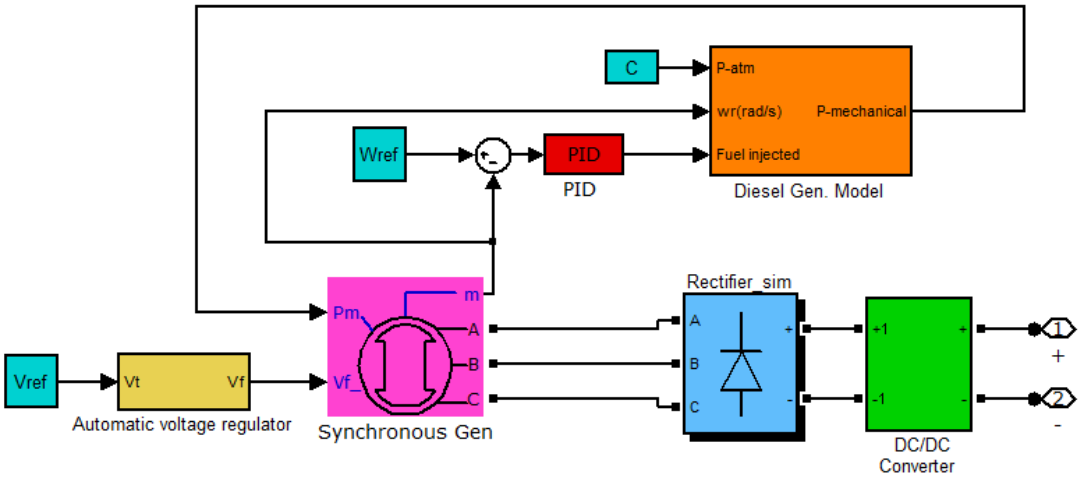

Figure 7. MatLab/SimPowSys simulation diagram of the DG model

2.4 Battery Energy Storage System (BSS)

The SimPowSys™ [33] model of lead-acid battery is used. Equations 3 and 4 illustrate the main relations used in the model.

$$E_{batt} = E_0 - K\frac{Q}{Q-it} + Ae^{-B.it} \quad (3)$$

$$V_{batt} = E_{batt} - R_{in} . I_{batt} \quad (4)$$

The state of charge of battery system (SoC-BSS) is estimated using the Equation (5)

$$SoC\_BSS = 1 - \frac{1}{Q}\int_0^t I_{batt}\, dt \quad (5)$$

Where A is the exponential-zone (V), B is the exponential-zone time constant inverse (Ah-1), E_{batt} is no-load voltage (V), is E_0 is battery constant voltage (V), I_{batt} is battery-charging and discharging current (A), K is polarisation voltage (V), Q is battery Ah, it is extracted capacity (Ah), R_{in} is internal resistance (Ω), Vbatt is terminal voltage (V). BSS is connected with the DC bus via DC/DC bidirectional converter as shown in Figure 9, it is controlled by the proposed energy management control strategy to keep the DC bus voltage within the specified range (380-420V).

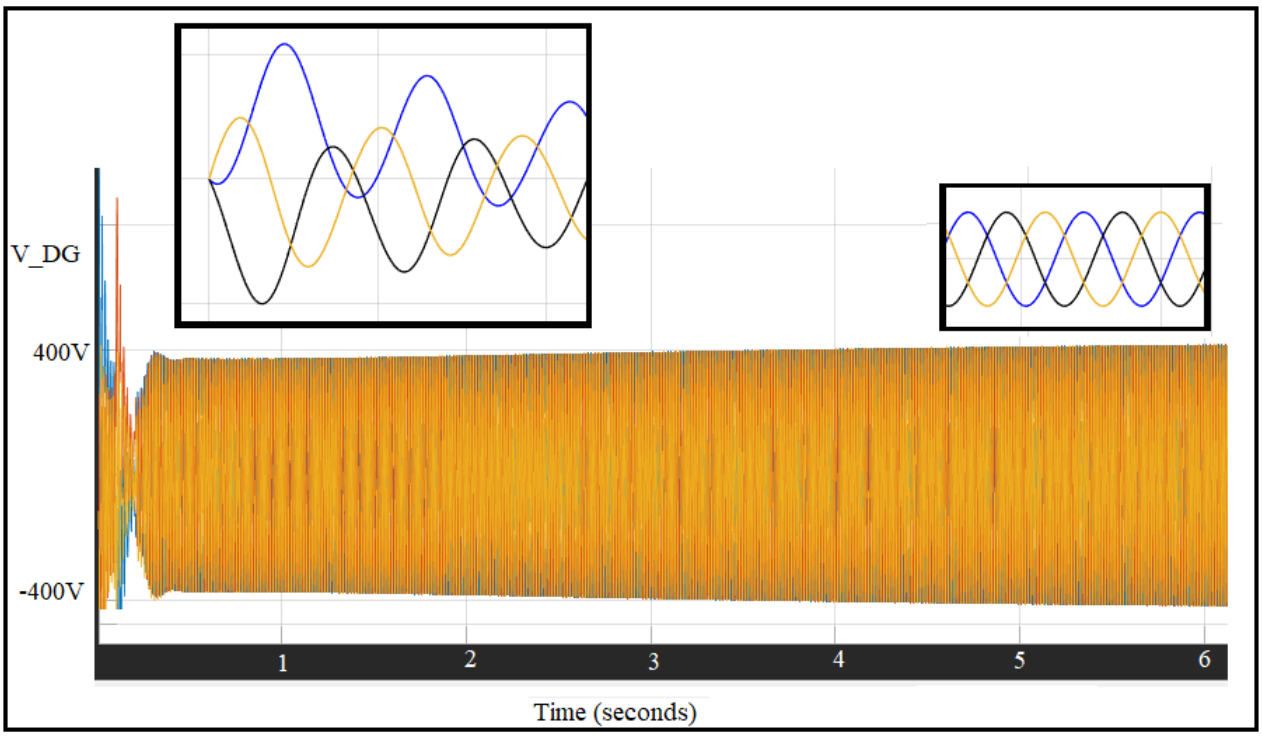

Figure 8: Validation of the DG model

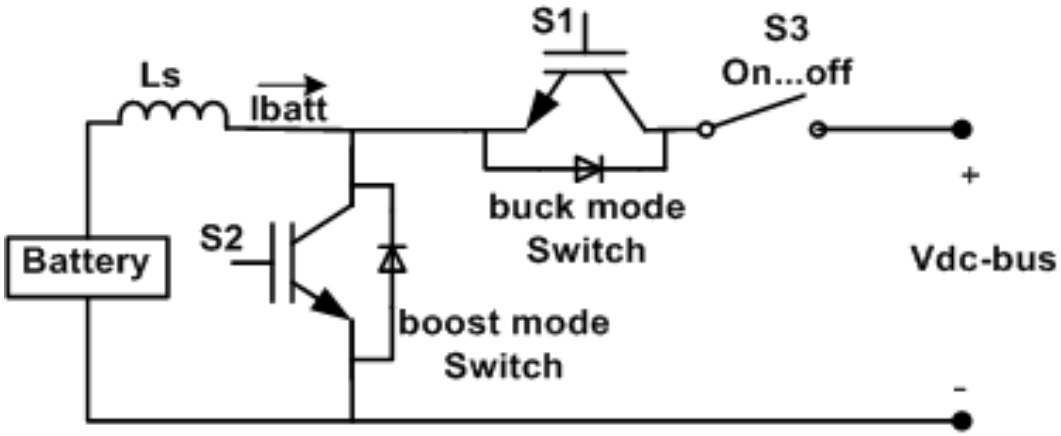

Figure 9. Bidirectional DC to DC converter with a schematic to the control strategy

2.5 Super-Capacitor SC

The super-capacitor is modeled in this study as internal resistance and a controlled voltage source [34]. The supercapacitor output voltage Vsc, supercapacitor current i_{sc} and self-discharge current i_{self_dis} are expressed using the following Equation (6) through (9):

$$V_{sc} = V_T - i_{sc} * R_{sc} \quad (6)$$

$$Q_T = \int_0^t i_{sc}\, dt \quad (7)$$

$$Q_T = \int_0^t i_{self\_dis}\, dt \;\; @ \;\; i_{sc} = 0 \quad (9)$$

Where V_T is the stern equation which is a function of the number of parallel and series supercapacitors, electric charge Q_T, the permittivity of a material, operating temperature, number of electrode layers, Interfacial area between electrodes and electrolytes [34]. The satate of charge of SCs (SoC-SC) is calculated using the Equation (10):

$$\text{SoC\_SC} = \frac{Q_{initial} - \int_0^t i(t)dt}{Q_T} \quad (10)$$

Where $Q_{initial}$ is the initial amount of supercapacitor electric charge and $i(t)$ is a function of supercapacitor current and self-discharge current. Figure 10 shows the behavior of

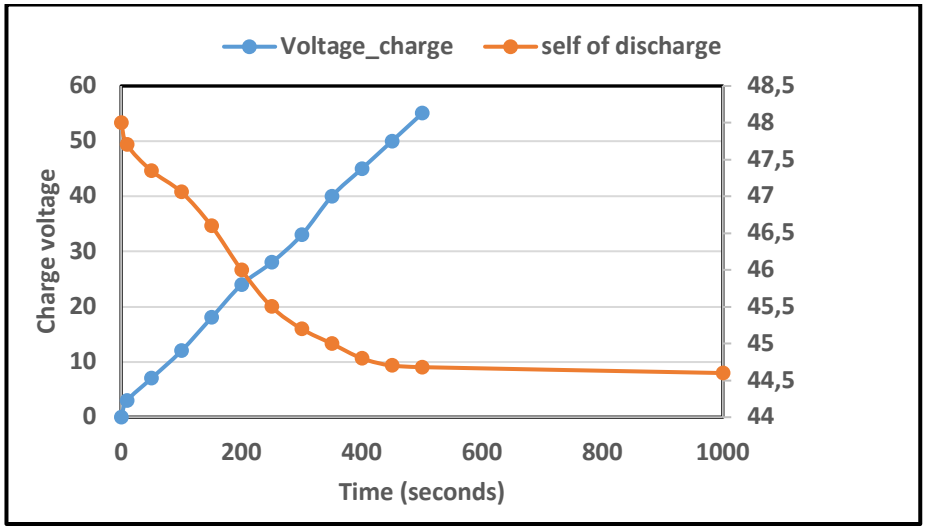

Figure 10: Voltage of Supercapacitor during charging and self of discharging

supercapacitor voltage during charging and self of discharging. The rated capacitance of the supercapacitor is 99.5F and the rated voltage is 48V.

2.6 Dump Load (DL)

The dump load rated power is selected to be 30% more than RES rated output power. The DL is connected to the DC bus.

3. Power Management Strategy

The aim of the management strategy is to ensure the continuity of power supply to load under different circumstances and effectively balance the power flow of PVEG, WEG, BSS, and backup systems. Balancing the power between the source and the load will maintain DC-bus voltage. Figures 11.a and 11.b show a flow diagram of the proposed power management strategy. It begins by estimating Pnet the difference between the power generated from RES and the load power demand as shown in Equation (11):

$$P_{net} = P_{PVEG} + P_{WEG} - P_{load} \qquad (11)$$

where P_{PVEG} and P_{WEG} are the power generated from PVEG and WEG, respectively. P_{load} is the load power. The power management strategy is mainly based on two operational modes: excess power mode and deficit power mode. The control strategy estimates the controlling current of BSS (i_{BSS}). The controlling current is called charging (i_{CBSS}) at excess power mode and called discharging (i_{DBSS}) at deficit power mode. The energy management strategy classifies the SoC-SC and SoC-BSS according to Table 2.

Table 2 Values and limits of SC and BSS state of charges

Classification		
Empty	SOC-SC ≤ 49%	SOC-BSS ≤ 49%
Full-min	85%>SOC-SC > 49%	85%> SOC-BSS > 49%
Full-max	SOC-SC = 90%	SOC-BSS = 85%

The third mode is when the generated power equals to load demand. It is rarely happened and not considered in the analysis, because wind speed, solar radiation, and load demand are always variable with time.

3.1 Excess power mode

The excess power mode is illustrated in Figure 11.a. If the energy generated from PVEG and WEG is greater than the required power from the load (P_{net}>0). This mode may be classified as normal excess or high excess. The control strategy estimates the controlling charging current of BSS (i_{CBSS}). In this study, the maximum charge current of BSS is 5A. If $i_{CBSS} \leq 5A$ the mode is classified as normal excess power while it is high excess power if the i_{CBSS}>5A. This classification is important because technically not recommended to charge the BSS with current greater than i_{CBSS}. There are five different cases in this mode. Some cases may be repeated but at different circumstances, as illustrated in the flow chart shown in Figure 11.a.

Case 1: Charge BSS

If the excess power is normal and SC is not empty (full-min

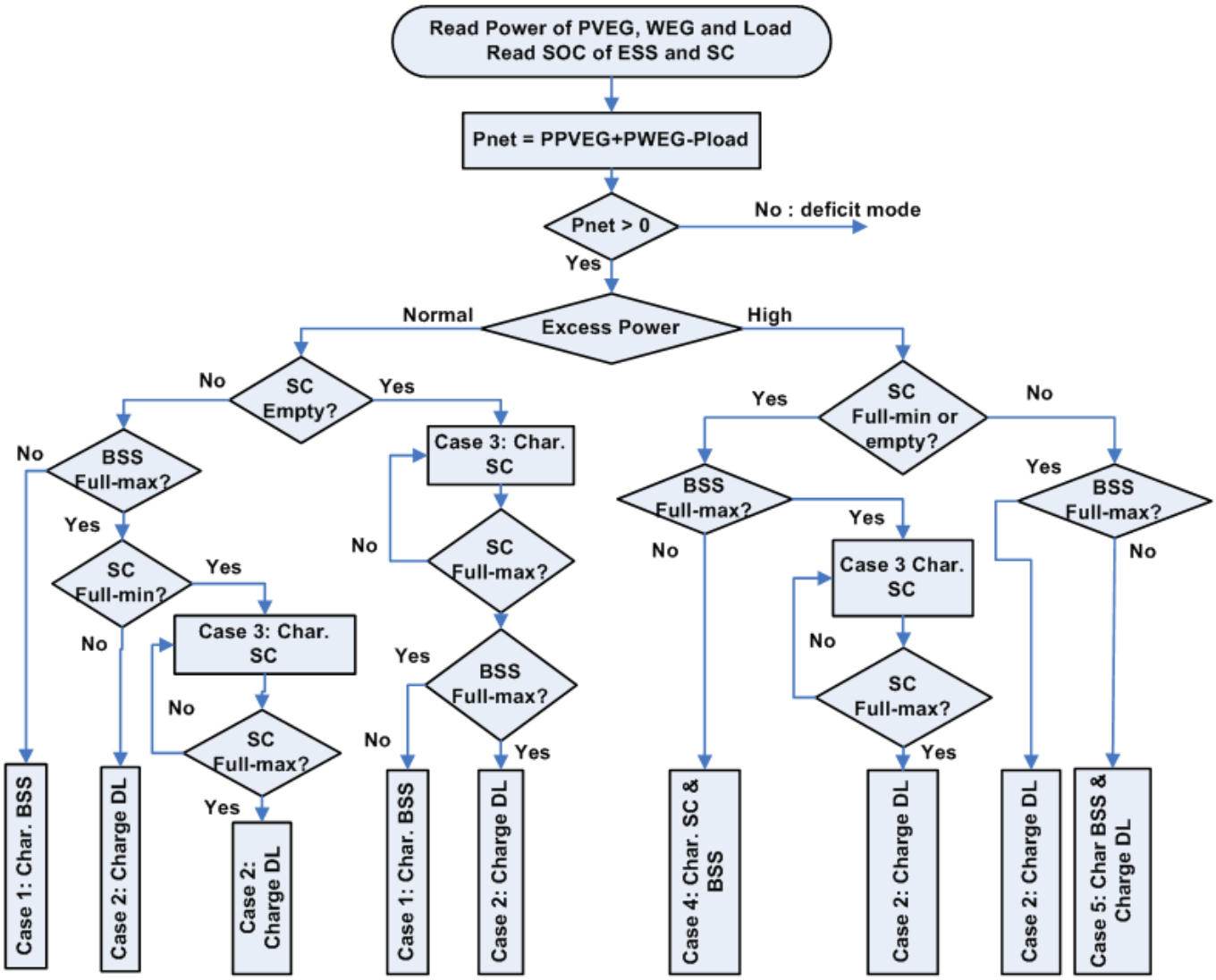

Figure 11.a. Flow chart of the energy management strategy at excess power mode

or full-max) and BSS is not full-max, then the surplus energy is injected to BSS until it becomes fully charged.

Case 2: Charge DL

This case is repeated five times in the energy management strategy, in all cases, the energy is injected to DL if the BSS and SC are full-max and the excess power is normal or high.

Case 3: Charge SC

This case is repeated various times as shown in Figure 16. The SC is charged if the BSS is full-max and the SC is full-min at normal excess power. The energy is also injected to SC if the SC is empty at normal excess power. If the BSS is full-max and SC is not full-max (empty or full-min), then the energy is injected to SC at high excess power mode.

It is good practice to take care of the problem of frequent charging and discharging of SC as a result of the fast self-discharge of SC [32]. Normally, the strategy keeps charging SC until SoC-SC becomes full-min. As a result of the fast self of discharging of SC, the SoC-SC becomes less than full-min within several seconds so frequent charging and discharging is taken place. In order to overcome this problem, the strategy use full-min and full-max classifications as illustrated in Table 2. At least 5% difference between the state of charge of full-min and full max. Now, the strategy keeps charging SC until reaching full-max. In this case, the SOC-SC needs several minutes to reach full-min instead of several seconds. So this hinders the SC from frequently charging and discharging.

Case 4: Charge SC and BSS

If the excess power is high, then the energy is required to be injected to BSS and SC if the SoC-BSS and SoC-SC are full-min or empty. It is good to note that SC will be charged until reaching full-max as indicated in case 3.

Case 5: Charge BSS and DL:

If the excess power is high and SoC-BSS is not full-max and SoC-SC is full-max, then the energy is injected to BSS and DL.

3.2 The deficient power mode

The excess power mode is illustrated in Figure 11.b. If the energy generated from PVEG and WEG is less than the required power from the load (P_{net} <0). This mode may be classified as a normal deficit or a high deficit. The

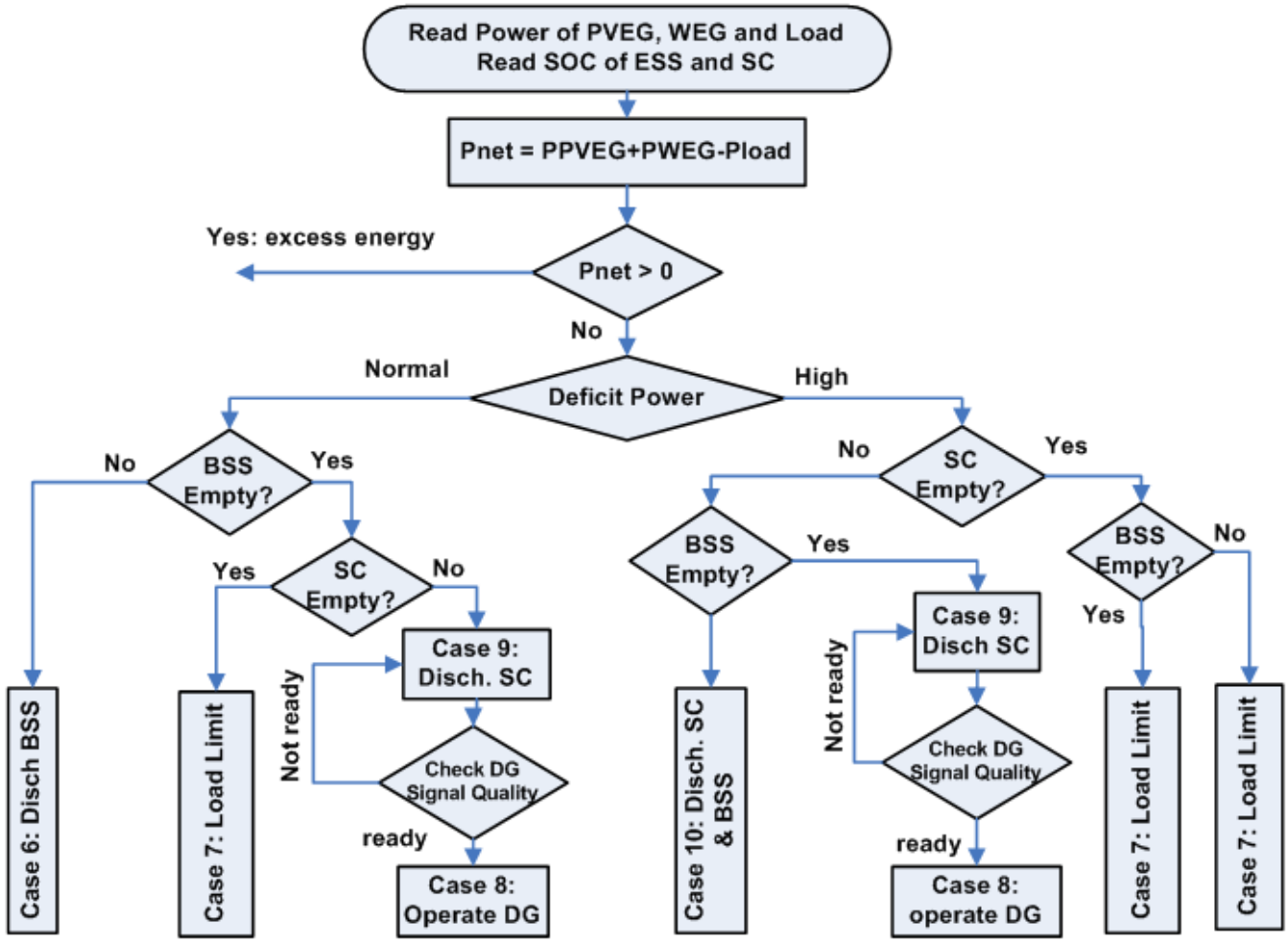

Figure 11.b. Flow chart of the energy management strategy at power deficiency mode

control strategy estimates the controlling discharging current of BSS (i_{DBSS}). In this study, the maximum discharge current of BSS is -5A. If $i_{DBSS} \geq -5A$ the mode is classified as normal deficit power while it is high deficit power if the $i_{DBSS} < -5A$. This classification is important because technically it is not recommended to discharge BSS at a current greater than i_{DBSS}.

Case 6: Discharge BSS

If the power deficit is normal and the SoC of BSS is not empty, then the BSS covers the deficit power.

Case 7: load limit

This case is repeated various times in the energy management strategy, but with different conditions and circumstances. If the deficit power is normal or high, BSS and SC are empty then the load is partially covered to be equal to the energy generated from PVEG and WEG. If the deficit power is high, SC is empty, BSS is not empty then the load is partially covered to be equal to the energy generated from PVEG, WEG, and BSS.

Case 8: Operate DG

When the BSS is empty and a normal or high power deficit occurs. In this case, the DG is utilized. Due to the sluggish dynamic behavior of DG, the DC-bus suffers from fluctuations during the startup of the DG. The SC is used to stabilize the DC-bus and compensate for the power deficiency [35], So the SC must be not empty before using DG.

Case 9: Discharge the SC

This case is an extension to case 8. The SC is discharged until the power signal from DG reaches stability. This case occurs if the power deficiency is normal or high, BSS is empty and SC is not empty.

Case 10: Discharge the SC and BSS

This case happens when the power deficiency is high, BSS and SC are not empty then the energy will be injected from SC and BSS to support PVEG and WEG to cover the deficiency.

4. Simulation Results and discussions

Figure 12 shows the simulation model. It shows the PVEG model connected to the DC bus through the DC/DC converter.

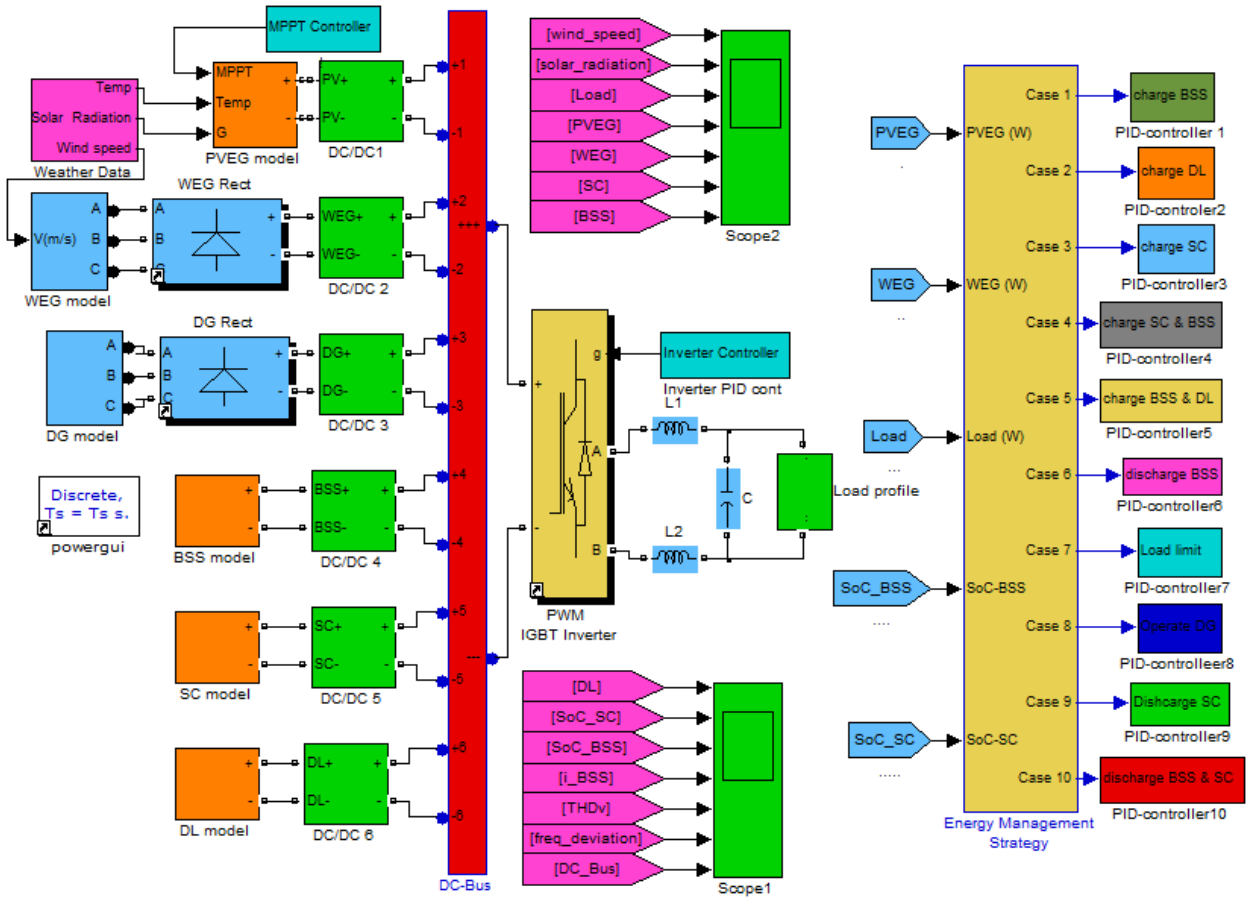

Figure 12. MatLab/Simulink/SimPowSys simulation model of stand-alone DC microgrid power system

The converter is controlled to extract maximum power from PVEG. WEG and DG are connected through the AC/DC rectifiers and DC/DC converters. The BSS and SC are connected through bidirectional DC/DC converters. The converters are controlled based on the energy management control strategy which aims to keep the DC-bus with the accepted range and balance the power flow. The converters control signals are controlled using PID controllers. The objective of the simulation tests is to confirm the effectiveness of the proposed energy management strategy using performance indexes: the frequency deviation, the stability of the DC bus voltage and the Total Harmonic Distortion of the voltage signal (THDv). The effective distribution of the required energy to the different power sources is another indicator of the effectiveness of energy management strategy. The measured quantities throughout the simulations are generated power from PVEG, WEG, and DG. The energy goes or comes from BSS and SC systems. The SoC-BSS and SoC-SC are measured as well. The charging i_{CBSS} and discharging i_{DBSS} controlling current of BSS is estimated.

Two cases are considered, dealing with different weather data and load demand day profiles. The ambient temperature is assumed to be constant (25°C) throughout the simulations. The solar radiation is expressed in per unit at base value 1kW/m^2, the assumed maximum and minimum solar radiation is 600 and 0 W/m^2, respectively. The wind speed is expressed in the actual values, the assumed maximum and minimum wind speed is 9 and 0 m/s, respectively. the power flow and load demand are expressed in the per-unit system at base value 1kW. The DC bus voltage is normalized at 400V. The normalized frequency deviation, that is computed as shown in Equation (12):

$$\Delta f=(f-f_r)/f_r \qquad (12)$$

where: fr is the grid rated frequency (50 Hz) and f is the actual frequency. The variation of the DC bus voltage level is considered as a further system stability index. In general, voltage variations are caused by sudden changes in the load or weather conditions. The DC bus voltage is controlled to remain within the 380 – 420V range. THDv is an index to take into account when evaluating the quality of the output AC voltage.

4.1 Simulation set 1

The time duration of the simulation set 1 in 110 minutes. The study proposes that SoC-BSS is full-max and the SoC-SC is empty at the beginning of the simulation. The proposed solar radiation input data and wind speed data are shown in Figure 13.a. The corresponding energy generated from PVEG and WEG during this period is illustrated in Figure 13.b. The load profile demand is shown in Figure 13.b. The charging/discharging energy of BSS and SC is shown in Figure 13.c in addition to the dumped energy. Figure 13.d shows the SoC-BSS and SoC-SC in addition to the i_{DBSS} and i_{CBSS}. In fact, the effect of energy flow from/to BSS and SC is reflected in the amounts of SoC-BSS and SoC-SC. Figure 13.e shows the THDv and frequency deviation in addition to the normalized DC-bus voltage. The simulation test is divided into six intervals:

Interval (0-10minutes): The average wind speed is about 7m/s, solar radiation is 0.35pu and the average load is 0.7pu. PVEG generates 0.6pu, WEG generates 0.38pu, so the generated energy is (P_{net}>0). The excess power is normal because $i_{CBSS} < 5A$. This is case 3 where the energy is injected to SC. The SoC-SC is increased in this interval from 0.48 to 0.52 as shown in Figure 13.d. During this period the DC-bus voltage keeps constant.

Interval (10-40minutes): The wind speed increases to 9m/s, the solar radiation increases to 0.6pu, the average load keeps constant at the first 10 minutes and increased slightly to 0.76pu from the 20th to 40th minutes. The high excess power mode occurs because $i_{CBSS} > 5A$. As the SoC-BSS and SoC-SC are not full-max, the power is injected to BSS and SC. Refer to the case 4 in the flow chart shown in Figure 11.a. The SoC-BSS and SoC-SC increase as shown in Figure 13.d. The DC bus voltage exceeds 400V but still within the accepted range, this increase is due to surplus power production.

Interval (40-50minutes): The wind speed and the load keeps constant, but solar radiation reduces to 0.3pu. The normal excess power mode occurs because $i_{CBSS} < 5A$. The SoC-SC is full-min and SoC-BSS is full-max. This is case 3 where excess power is injected to SC. Figure 13.d shows an increase in SoC-SC while SoC-BSS keeps constant.

Interval (50-60minutes): The wind speed and solar radiation keep constant, but the load demand increases to 1.48pu. The deficit power is high because $i_{DBSS} < -5A$. The SoC-SC and SoC-BSS are not empty. This is the case 10 where deficit power is compensated from SC and BSS. Figure 13.d shows a decrease of SoC-SC and SoC-BSS. The DC bus reduces in this period to 0.95 PU but still within the range.

Interval (60-70minutes): The wind and solar radiation keep constant, but the load reduces to 1.08pu. The deficit power is normal because $i_{DBSS} > -5A$, so BSS compensates the deficit and SC is off. This is in case 6. The SoC-BSS is decreased as a result of its contribution to balance the energy flow. The SoC-SC is slightly decreased from 0.69 to 0.68 as a result of the self of the discharging effect.

Interval (70-80-90-100minutes): The wind speed and solar radiation increase to 8m/s and 0.6pu, respectively. The load fluctuates during this period but the excess power is high as the generated power from PVEG and WEG more than the required load. The SoC-SC and SoC-BSS are not full-max and $i_{CBSS} > 5A$, then the surplus energy is injected into SC and BSS. As a result, the SoC-SC and SoC-BSS rise. This is case 4 as illustrated in the flow chart shown in Figure 11.a. During this period, the DC voltage fluctuates within the accepted range.

Interval (100-103minutes): The excess power during this small period is still high. The SoC-BSS is full-max and SoC-SC is still full-min. This is case 3 where the energy is injected to SC.

Interval (103-110minutes): The excess power is high as $i_{CBSS} > 5A$ and the SoC-BSS and SoC-SC are full-max. This is case 2, where the energy is injected into DL. It is good practice to note the effect of self of discharging of SC in this period. The SoC-SC has reduced by about 0.01 even the SC is off. Furthermore, the SoC-SC becomes less than full-max and case 2 still runs without converting to case 3 where the surplus energy should be injected to SC. In fact, this is good because it prevents SC from frequent charging and discharging.

The system is steady during all the considered intervals as it is likely to note from the Δf chart. The normalized frequency deviation is always less than 0.01. The DC bus voltage remains constant around 1pu except for the period between (50 -70) minutes it fluctuates between 1 and 0.96pu which is still within the allowed range of variation. In general, The DC-bus voltage fluctuates when transferring between cases, it exceeds 1pu at excess power modes and reaches 0.97pu at deficiency power modes. The objective of the control strategy and PID controllers is to keep the DC-bus voltage within the accepted range. The overall results of the simulation ensures that the control strategy hineders the frequent charging and discharging of the SCs and BSS.

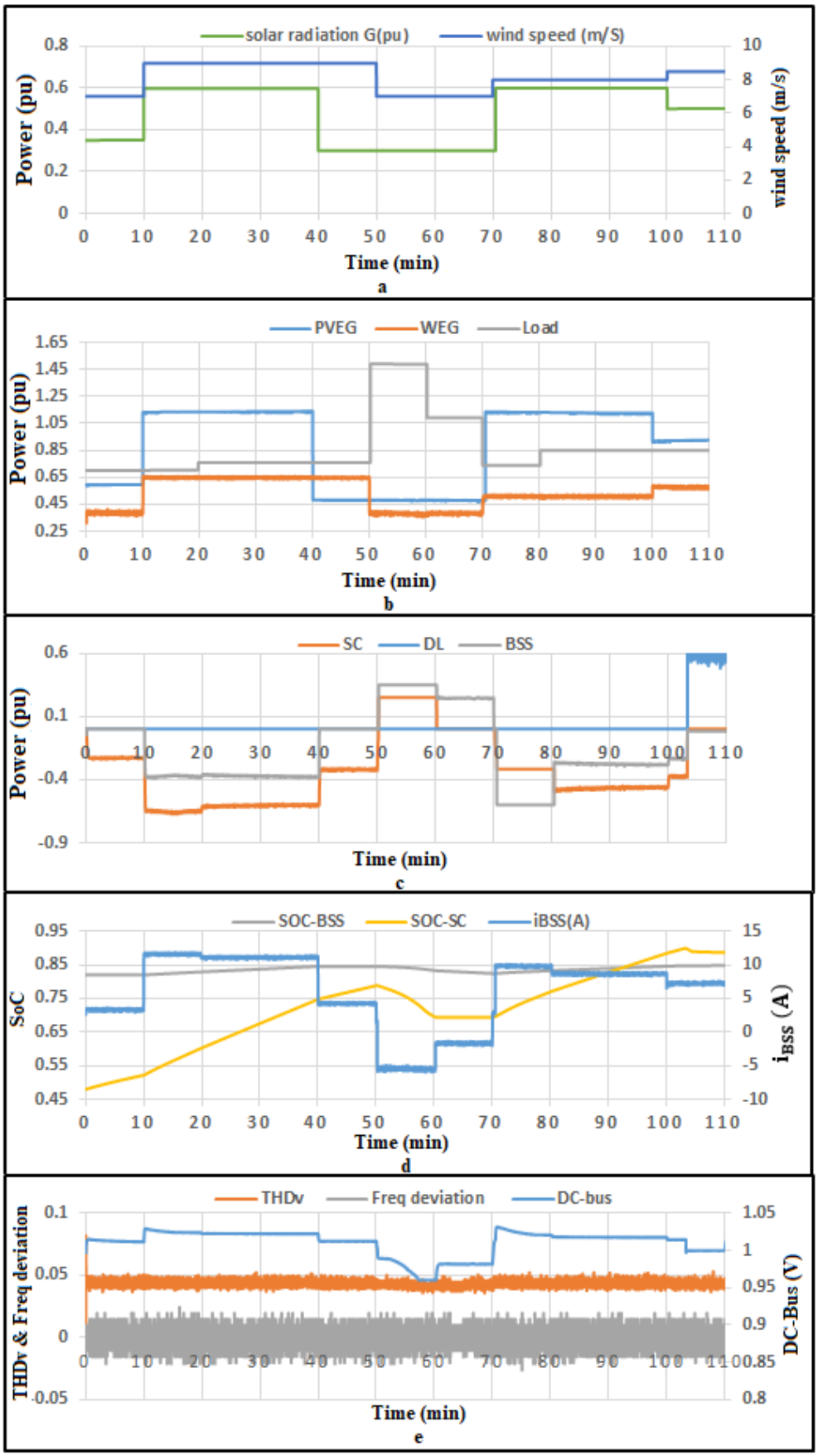

Figure 13. Results of simulation set 1: (**a**) wind speed and solar radiation input data; (**b**) energy generated from PVEG, WEG and required load; (c) energy from/to SC and BSS, energy generated from DG and energy injected to DL; (d)Controlling current (A) SoC-SC and SoC-BSS; (e) THDv, frequency deviation and DC-Bus(pu)

4.2 Simulation Set 2

The time duration of simulation set 2 in 80 minutes. The study proposes that SoC-BSS is empty and the SoC-SC is full-max at the beginning of the simulation. Figures from 14.a through 14.e show the detailed results of the simulation set 2 at the same arrangement of simulation set 1. The simulation test can be divided into five intervals:

Interval (0-10minutes):
The solar radiation in this period is zero, the wind speed is 7m/s. The energy generated from WEG is 0.38pu and the load is 0.7pu. The power from WEG is insufficient to support the load and the deficit power is normal (i_{DBSS} > -5). The SoC-BSS is empty so the DG take the lead to cover the deficiency, this is the case 8. Because of the slow dynamic of DG, it can't enter the system instantaneously, it needs several seconds until reaches stability. During this period the SC compensates the deficiency and keeps the DC-bus within the required rates (380-420V). After approximately one minute, the DG starts operation. This is illustrated in Figure 14.c. Figure 19.d shows how SoC-SC is reduced.

Interval (10-20minutes):
This is an extension to case 8 as the DG still takes the lead but at higher power. The generated power from WEG is reduced and load demand increases consequently the deficiency is high (i_{DBSS} < -5). The DG continues to support the load without interruption or interference from SC. Figure 14.c shows how the power generated from DG increases. Figure 14.d shows how SoC-SC decreases as a result of the self of discharging only.

Interval (20-30minutes):
In this period the solar radiation reaches 0.4pu. The power generated from PVG and WEG is greater than the required load. The excess power is normal (i_{CBSS} < 5), the SC is full-max, BSS is not full-max. So the energy management strategy injected the surplus power to BSS. Refer to case 1 in the flowchart shown in Figure 11.b. Figure 14.c shows that SoC-BSS increases as a result of energy injection to BSS and SoC-SC decrease as a result of self of discharging.

Interval (30-70minutes):
The power generated from PVG and WEG is still greater than the required load, but excess is high. The SC is full-max, BSS is not full-max. So the energy management strategy injected the surplus power to BSS and DL. Refer to case 5 in the flowchart shown in Figure 11.b. Figure 14.c shows the amount of surplus energy injected to DL. Figure 14.d shows that SoC-BSS increases as a result of energy injection to BSS and SoC-SC decrease as a result of self of discharging.

Interval (70-80minutes):
The wind speed is 0m/s and the load is 0.8pu. The power generated from PVEG is slightly insufficient to provide the load, so the deficit power is normal. The BSS compensates the deficit. This is in case 1.

The system is steady during all the intervals as it is likely to note from the Δf chart. The normalized frequency deviation is always less than 0.02 in the simulation set 1. The DC bus voltage remains around 1pu. The period from 0 to 20minutes represents power deficiency and involving operating DG, the DC-bus fluctuates and reaches 0.96pu. The period from 20 to 60minutes represents excess power and the DC-bus voltage reaches 1.02pu. The period from 60 to 70minutes represents power deficiency and this the reason why DC-bus voltage reduces to 0.98pu. The fluctuations are within the permitted range of variation. Moreover, the AC voltage THDv does not exceed 0.04, which is a standard requirement [36], all over the simulation set 1and 2.

5. Conclusions

A stand-alone DC microgrid based on WEG, PVEG, BSS, and DG combined with SC is proposed. All components are modeled using Matlab/Simulink / SimPowSys^{TM} environment and a complete model is designed using the same environment. The energy management strategy is programmed using a deterministic approach.
Two simulation sets have been implemented to check the consistency of the developed strategy in different operating conditions. The energy management strategy includes 10 cases that simulate truly real situations. The results show that the proposed control strategy is able to regulate the DC bus voltage within acceptable limits. A power balance is verified even with the intermittent power output nature of WEG and PVEG. Obtained results confirm the effectiveness of the proposed energy management strategy and considered as a basis for a practical realization.
The results show that DG is a good back up power source after BSS is used up. The DG can't immediately couple with the DC-bus because of its sluggish dynamic behavior. The energy management strategy utilizes SC to overcome this problem as it has a fast response and high power density.
The energy management strategy utilizes SC to manage to charge and discharging of the BSS in case of high power deficiency and high excess power. The strategy overcomes the problem of frequent charging/discharging of the SC. The strategy considers a dumping load to keep the balance in the DC-Bus during excess power cases.
The results obtained from simulating such complicated system add value to the bulk of science in the field of modeling and energy management of standalone systems, which is, in fact, the main aim of this paper.

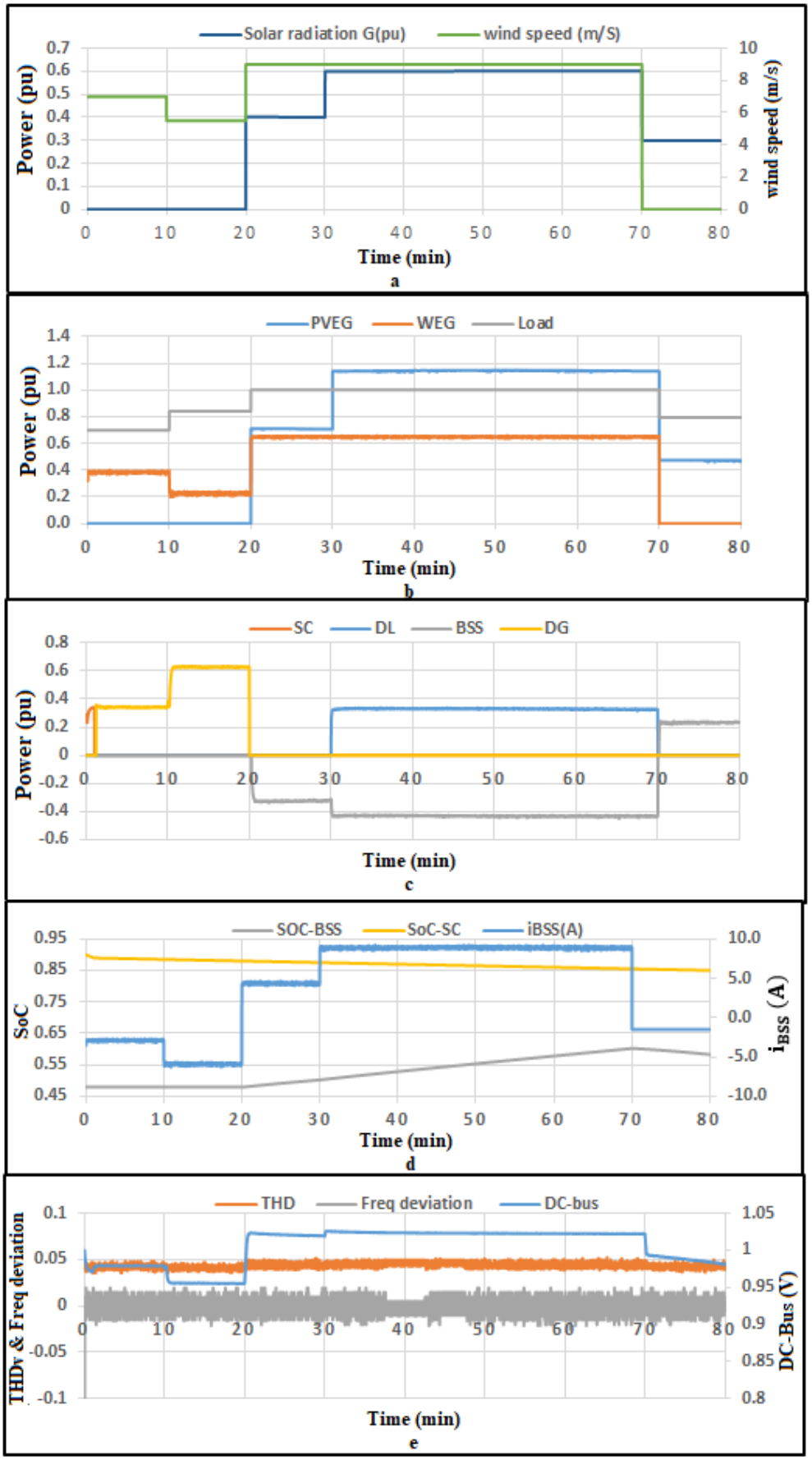

Figure 14. Results of simulation set 2: (**a**) wind speed and solar radiation input data; (**b**) energy generated from PVEG, WEG and required load; (c) energy from/to SC and BSS, energy generated from DG and energy injected to DL; (d) Controlling current (A) SoC-SC and SoC-BSS; (e) THDv, frequency deviation and DC-Bus(pu)

References

[1] H. Hui, N. Xie, D. Fang, and X. Zhang, ''The role of renewable energy consumption and commercial services trade in carbon dioxide reduction: Evidence from 25 developing countries'', Applied energy, vol. 211, pp. 1229-1244, 2018

[2] E. Hossain, E. Kabalci, R. Bayindir, R. Perez, ''Microgrid testbeds around the world:state of art'', Energy Conversion Management, vol. 86, pp.132–53,2014.

[3] M. Longo, W. Yaïci and F. Foiadelli,'' Hybrid Renewable Energy System with Storage for Electrification – case study of remote northern community in Canada'', International Journal of Smart Grid, Vol.3, no.2, june, 2019

[4] G. Chicco and P Mancarella, ''Distributed multi-generation: a comprehensive view'', Renewable and Sustainable Energy Reviews ;vol. 13(3), pp. 535–51, 2009.

[5] C. Yin , M Sechilariu , F Locment, ''Diesel generator slow dynamic compensation by supercapacitors for DC microgrid power balancing'', ENERGYCON IEEE Int. Energy Conference, pp. 1–6, 2016.

[6] E. Planas, J. Andreu, JI. Gárate, A. Martínez I, E. Ibarra, ''AC and DC technology in microgrids: a review'', Renew Sustain Energy Rev ;vol. 43, pp. 726–49, 2015.

[7] T. Baba , Y. Mizuno, K. Fujio, Y. Tanaka znd N. Matsui,''Evaluation of An Island Operation Method Smart Grid Using A Power Emulation System''International Conference on Smart Grid (icSmartGrid) IEEE, 2018.

[8] Von Meier, Alexandra. Electric power systems: a conceptual introduction. John Wiley & Sons, 2006.

[9] Eghtedarpour, Navid, and E. Farjah. "Distributed charge/discharge control of energy storages in a renewable-energy-based DC micro-grid." IET Renewable Power Generation, vol. 8.1, pp. 45-57, 2014

[10]AT. Elsayed, AA. Mohamed, QA. Mohammed,'' DC microgrids and distribution systems: an overview'', Electr Power Syst Res, vol. 17,pp. 119-407, 2015.

[11] Yu Shimizu and H. Kitano, ''Exchangeable batteries for micro EVs and renewable energy Taichiro Sakagami'', IEEE 6th International Conference on Renew able Energy Research and Applications (ICRERA), 2017 Year: 2017 | Conference Paper | Publisher: IEEE

[12] T. Sakagami; Yu Shimizu ; H. Kitano,'' Exchangeable batteries for micro EVs and renewable energy'', 6th International Conference on Renewable Energy Research and Applications (ICRERA) IEEE, Nov. 2017

[13] S. Das, AK Akella, ''Power flow control of PV-wind-battery hybrid renewable energy systems for stand-alone application'' International Journal of Renewable Energy Research (IJRER), vol. 8(1), pp. 36-43, 2018.

[14] C. Yin, H. Wu , F. Locment, M. Sechilariu, "Energy managgement of DC microgrid based on photovoltaic combined with diesel generator and supercapacitor." Energy conversion and management, vol. 132, pp. 14-27, 2017.

[15] Z. Roumila, D. Rekioua,T. Rekioua."Energy management based fuzzy logic controller of hbrid system wind/photovoltaic/diesel with storage battery." International Journal of Hydrogen Energy, vol. 42.30,pp. 19525-19535, 2017.

[16]M. Kumar, SC. Srivastava, SN. Singh,'' Control strategies of a DC microgrid for grid connected and islanded operations'', IEEE Trans Smart Grid,vol. 6, pp. 1588–601, 2015.

[17]AM. Dizqah, A. Maheri, K. Busawon, A. Kamjoo, "A multivariable optimal energy management strategy for standalone dc microgrids." IEEE transactions on power systems, vol. 30.5, pp. 2278-2287, 2014.

[18] Y. Han, W. Chen, Q. Li, H. Yang, F. Zare, Y. Zheng . "Two-level energy management strategy for PV-Fuel cell-battery-based DC microgrid." International Journal of Hydrogen Energy, vol. 44.35, pp. 19395-19404, 2019.

[19] RK Sharma, S Mishra, "Dynamic power management and control of a PV PEM fuel-cell-based standalone ac/dc microgrid using hybrid energy storage." IEEE Transactions on Industry Applications, vol. 54.1, pp. 526-538, 2017.

[20] Z. Cabrane, M. Ouassaid, and M. Maaroufi, "Battery and supercapacitor for photovoltaic energy storage: A fuzzy logic management," IET Renew. Power Gener., vol. 11, no. 8, pp. 1157–1165, 2017

[21] A. Iovine , T. Rigaut, G. Damm , E. De Santis, MD. Di Benedetto, ''Power management for a DC MicroGrid integrating renewables and storages'', Control Engineering Practice, vol. 85, pp. 59-79, 2019.

[22] Z. Ye, JJ Hong, G. Li, ''Energy management strategy of islanded microgrid based on power flow control'', IEEE PES Innovative Smart Grid Technologies (ISGT) conference, Washington, DC, pp. 1–8, 2012.

[23] E. Muljadi, S. Drouilhet, R. Holz and V. Gevorgian, ''Analysis of permanent magnet generator for wind power battery charging'', IEEE Industry Applications Conference, pp. 541 -548, 1996.

[24] JF Manwell, JG McGowan, AL Rogers. Wind energy explained: theory, design and application. John Wiley & Sons; 2010 Sep 14.

[25] A. Belkaid, I Colak, K. kayislic, and R Bayindird, '' Modeling of a Permanent Magnet Synchronous Generator in a Power Wind Generation System with an Electrochemical Energy Storage'', International Journal of Smart Grid, Vol.2, No.4, December, 2018

[26] S. Benhamed and etal,'' Dynamic modeling of diesel generator based on electrical and mechanical aspects'', IEEE Electrical Power and Energy Conference (EPEC), pp. 1-6, October 12, 2016

[27] JT. Bialasiewicz, E. Muljadi, S. Drouilhet, G. Nix,'' Hybrid power systems with diesel and wind turbine generation'', American Control Conference, Vol. 3, pp. 1705-1709, 1998.

[28] AA. Adesanya and S. Chelsea, "Solar PV-diesel hybrid systems for the Nigerian private sector: An impact assessment." Energy Policy, vol. 132, pp. 196-207, 2019

[29] C. Ghenai and M. Bettayeb, "Modelling and performance analysis of a stand-alone hybrid solar PV/Fuel Cell/Diesel Generator power system for university building." Energy, vol. 171, pp. 180-189, 2019.

[30] S. Yilmaz and D. Furkan, "Optimal design of hybrid PV-Diesel-Battery systems for isolated lands: A case study for Kilis, Turkey." Renewable and Sustainable Energy Reviews, vol. 77, pp. 344-352, 2017.
[31] L. Xu, D. Chen, ''Control and operation of a DC microgrid with variable generation and energy storage'', IEEE Trans Power Deliv, vol. 26, pp. 2513–22, 2011.
[32] A. Etxeberria, I. Vechiu, H. Camblong, JM. Vinassa,'' Comparison of three topologies and controls of a hybrid energy storage system for microgrids'', Energy Convers Manage, vol. 54, pp. 113–21, 2012.
[33] O. Tremblay, L.A. Dessaint, "Experimental Validation of a Battery Dynamic Model for EV Applications." World Electric Vehicle Journal. Vol. 3, May 13–16, 2009.
[34] N. Xu and J. Riley, "Nonlinear analysis of a classical system: The double-layer capacitor," Electrochemistry Communications, vol. 13, no. 10, pp. 1077-1081, 2011.
[35] H. Yoo, S. Sul, Y. Park, J. Jeong. ''System integration and power-flow management for a series hybrid electric vehicle using supercapacitors and batteries'', IEEE Trans Ind Appl, vol. 44, pp. 108–14, 2008.
[36] IEEE Standards 519-1992, "Recommended Practices and Requirements for Harmonic Control in Electric Power Systems", 1992.